COMPARATIVE STUDIES ON THE HIGH TEMPERATURE OXIDATION BEHAVIOUR OF HAYNES 282 AND INCONEL 718 NICKEL-BASED SUPERALLOYS

*Bodude, M. A[1] and Nnaji, R. N[2]

[1,2.] Department of Metallurgical and Materials Engineering, University of Lagos,
Akoka, Lagos, Nigeria
*Corresponding Author: mbodude@unilag.edu.ng +234 805 558 6945

ABSTRACT:

Nickel-based superalloys are heat-resistant metallic materials used in aero- and land-based gas turbine engines hot sections. At high temperatures above 1000 °C, oxidation behaviour of gas turbine superalloy materials is characterized by the oxidation reaction rates and formation of stable and adherent oxide films on the materials' surfaces. However, superalloy materials display varying oxidation behaviours due to compositional differences and environmental conditions. In this present investigation, the high temperature oxidation behaviour of Haynes 282 and Inconel 718 nickel-based superalloys were examined through experimental study at both 1050 °C and 1100 °C test temperatures for maximum exposure periods of 10 hours (36000 seconds). The morphological, microscopic, and elemental compositions of the formed-surface oxides were assessed using Optical Light Microscopy, Scanning Electron Microscopy (SEM) and X-ray Energy Dispersive Spectroscopy (EDS). The parabolic oxidation rate constant, k_p was calculated from the slope of the best-fit straight lines for the plots of both superalloys experimental weight gain data at both test temperatures. As observed $k_p = 3.9 \times 10^{-2}$ (mg/cm². s) and 4.6×10^{-2} (mg/cm². h) for Haynes 282; and $k_p = 1.4 \times 10^{-2}$ (mg/cm². s) and 4.4 (mg/cm². s) for Inconel 718 at 1050 and 1100 °C test temperatures respectively. Haynes 282 had an overall higher weight gain and k_p than Inconel 718 under the same test conditions at both test temperatures as observed from the oxidation experiments. EDS results showed elemental presence of chromium and titanium oxides for Haynes 282; and predominantly elemental presence of chromium oxide for Inconel 718.

Keywords: Haynes 282, Inconel 718, Oxidation kinetics, Oxides, Superalloys.

INTRODUCTION

Superalloys are heat-resistant multi-component (15 elements or more) metallic materials designed for high temperature applications such as jet engines and power-generation gas turbines. Superalloys are classified into three main groups namely, iron-based, cobalt-based, and nickel-based. Superalloys premier introduction into military gas turbine engines in the second quarter of the 20th century (during World War II) led to significant improvement in jet engine production technology in the modern aerospace industry (Pérez-González *et al*., 2014; Barbosa *et al*., 2005). The largest application of superalloys is in the gas turbine industry, where good mechanical strength and thermal stability at service temperatures are required

(Shukla *et al.,* 2013). Intensive superalloy development and processing over the past few decades have resulted in nickel-based superalloys that can tolerate average temperatures of 1050 °C with occasional short trips (near airfoil tips) to 1200 °C (Pollock and Tin, 2006). The popularity of nickel-based superalloys in high-temperature applications is largely due to their high-temperature oxidation and creep resistance (Wu *et al.*, 2010).

Improved efficiency, which is the requirement for all types of modern gas turbines, often come with increased operating temperatures and increased risk of high-temperature oxidation of gas turbine components, especially turbine blades. For engine best performance, the combustion temperature should be the maximum obtainable from the complete combustion of the oxygen and the fuel (Eliaz *et al.,* 2002). The total power produced and the engine efficiency often depend on the condition of individual turbine blade. Therefore, the turbine blades must be capable of withstanding more demanding environments, which include high centrifugal stresses and very high temperatures. These severe operating conditions lead to fast degradation of the turbine blades, which ultimately weakens overall engine performance through mechanisms such as high-temperature oxidation (Saravanamutto *et al.*, 2009; Caron and Khan, 1999; Smith, 2013).

Gas turbine nickel-based superalloy components depend on formation of compact oxide layers to provide protection against high-temperature oxidation. However, a stable protective oxide may crack, spall or even form volatile compounds at temperatures above 1000 °C leading to loss in oxidation resistance. Thereby, significantly increasing the problem of high-temperature oxidation above this temperature; and consequently, formation of more stable oxides will be required at operating temperatures exceeding 1000 °C (Ahlatci, 1991; Mahobia *et al.*, 2013; Zitnansky *et al.*, 1998; ASM, 1997; Pomeroy, 2005; Smith, 2013). Previous studies on the isothermal oxidation behaviour of nickel-based superalloys reported different oxidation rates and growth of complex oxides between 800 – 1050 °C test temperature range but the proportions of the elements that combine to form the products (oxides) varies with the chemical composition of the base material, temperature, time, and the environment (Pérez-González *et al.*, 2014). Therefore, this study deals with the results obtained from the high temperature oxidation tests performed on Haynes 282 and Inconel 718 nickel-based superalloys at both 1050 and 1100 °C under isothermal conditions for a maximum exposure period of 10 hours.

MATERIALS AND METHODS

The Haynes 282 and Inconel 718 superalloys used in this study were obtained from Canada in their wrought forms. Rectangular specimens of approximate dimensions 11.0 mm x 8.0 mm x 4.0 mm were cut using a MARVEL (AB), Armstrong-Blum Mfg., Series 8, Mark II vertical band saw machine. Samples of both superalloys were cut to approximate dimensions of 10.6 mm x 8.0 mm x 4.0 mm. Samples were ground using 600, 800, and 1,200 grits in succession to remove all surface oxides and roughness. The samples were then cleaned by immersing them in methylated spirit for 10 minutes and thereafter, washed with hot water to remove any possible oil or residue contaminants deposited on the sample during the cutting and grinding processes. Samples were dried using hot air from a hand-held hair dryer.

The samples and ceramic crucibles were weighed before the oxidation experiments using a digital weighing scale (Shimadzu UW1020H) sensitive to 0.001g. Samples were placed in specific arrangements in the crucibles and then on a stainless-steel plate (secondary plate) and held in place by a mild steel plate (primary plate); subsequently placed inside a Vecstar PF muffle furnace Model with maximum temperature capacity of 1200 °C. Oxidation tests were conducted at 1050 and 1100 °C respectively in laboratory air for times up to 10 h (36000 s). The samples were placed in the furnace at ambient temperatures and heating continued at a heating rate of 5 °C/min until the furnace temperature stabilized at 1050 °C. The samples and crucibles were oxidized at 1050 °C for different exposure times ranging from 0 to 10 hours for either of both superalloys. Upon removal from the furnace, the oxidized weights of the samples and crucibles were taken using the same digital scale as above and weight gain was calculated. The experiment was performed two times and the average measurements were recorded. Oxidation tests at 1100 °C for Haynes 282 and Inconel 718 superalloy samples followed the same procedure above as described for the 1050 °C test temperature. Figure 1 (a and b) show the experimental set up, while Figure 2 (a and b) show the furnace stabilization at the first test temperature and furnace environment just before samples retrieval.
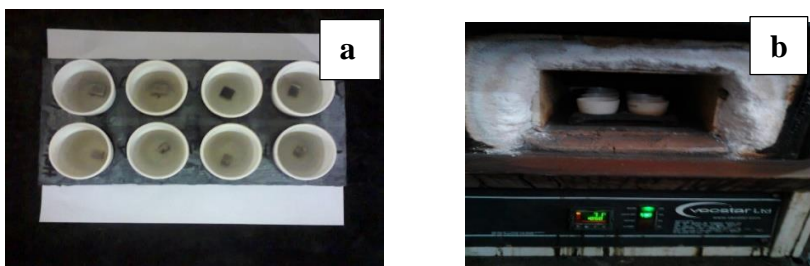

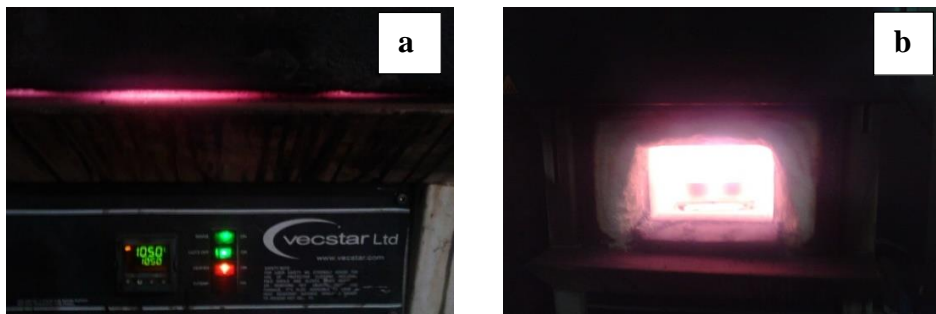*Figure 1: (a) samples arrangement inside the crucible; (b) crucible arrangement in the furnace.*

Figure 2: (a) furnace stability at first test temperature; (b) furnace environment before samples were retrieved.

Light Optical Microscopy (LOM)
Test samples were buffered with aluminium foil, cotton pads, and masking tape. Samples clamped to a table vice and carefully sectioned longitudinally using a hardened hacksaw steel blade for each cut. Samples cross sections were mounted in epoxy (resin). Surface grinding of mounted samples cross-sections was conducted with successive finer wet silicon carbide papers from 220 to 1200 grit. The edges were properly chamfered and rounded to ensure proper flat surfaces of the specimens during the grinding operations. Samples were then polished using 0.3 µm and 0.05 µm alumina slurries sequentially. They were subsequently washed under running water and dried using hot air from a hand-held hair dryer. They were chemically etched, washed again under running water, and dried using hot air from same dryer. The longitudinal cross-sectional areas of the oxidized specimens were examined using light optical microscope type [CETI] fitted with digital camera (5 Mega Pixels resolution) in the Laboratory at the Department of Metallurgical and Materials Engineering, University of Lagos. Samples of the as-received Haynes 282 and Inconel 718 superalloys were also subjected to the above metallographic procedures and etched for light optical microscopy.

Scanning Electron Microscopy (SEM) and Energy Dispersive X-Ray Spectroscopy (EDS)
To further examine the morphology and composition of the oxides formed, SEM and EDS were used. EDS was used to identify the elemental composition of the formed-oxides on the surface of the samples. For this investigation, the Phenom Desktop SEM machine with Phenom ProX software attached, in Covenant University, Ota, Ogun State, Nigeria was used.

Nickel-based superalloy materials form protective oxides such as Cr_2O_3 (chromia) when exposed to oxidizing environments at high temperatures. Often, the rate of formation of chromium oxide is quicker in comparison with other protective oxides. This makes chromium oxide a preferred oxide since it will form quickly to protect the alloy, and will repair itself quickly in the event of oxide layer spallation. However, chromium oxide may lose its protective properties at temperatures above 1000 ℃, leading to formation of volatile CrO_3. Consequently, Cr_2O_3 alone may not provide sufficient oxidation protection at very high temperatures (Cottis *et al.*, 2010; Smith, 2013)

RESULTS AND DISCUSSION
The average nominal compositions of the as-received Haynes 282 and Inconel 718 superalloys given by the PMI (Positive Material Identification) machine at Midwal Engineering and Testing Laboratory, Lekki, Lagos, Nigeria are shown in Table 1. Three locations on each alloy sample were x-rayed using the PMI machine and the averages were calculated as shown in the table.

Table 1: Average Nominal Composition of As-Received Haynes 282 and Inconel 718 Superalloys (wt. %)

Element	Ni	Cr	Fe	Nb	Mo	Ti	Al	Co	C	Mn	Si	P	S	B	Cu
Haynes 282	57.96	18.03	2.81	-	8.62	1.97	ND	9.40	ND	0.13	ND	-	-	-	ND
Inconel 718	50.08	18.98	18.95	5.03	3.14	1.00	ND	0.24	ND	0.09	ND	ND	ND	ND	ND

ND = Not Determined

Oxidation Performance and Weight Change
The entire surface area was used for the calculation of the weight change per area, which was approximately 0.85 cm² for both superalloy test samples. Most of the oxidation observed took place on the top surface exposed to the oxidizing environment as shown in the sample arrangement in Figure 1(a) and therefore, contributed the most to the weight gain of each sample (Olivares *et al*., 2013; Smith, 2013).

Weight change during a high temperature oxidation process has been reported to follow a relationship of the form:

$$\Delta W = k_p.t^{0.5} \qquad\qquad (1)$$

Where, ΔW represents the weight change per unit area in mg/cm², k_p the parabolic oxidation rate constant in mg cm^{-2} s^{-1}, and t is the oxidation time at a particular temperature in seconds. Eq. (1) implies that weight gain, (ΔW), is proportional to the square root of time ($t^{0.5}$) (Pérez-González *et al.,* 2014; Olivares *et al*., 2013; Sinharoy and Narasimhan, 2004). The experimental weight gain data was fitted according to the power law inside a time-window varying over the entire experiment period using the curve-fitting tools of OriginPro 8.5 of Origin Lab Software. The parabolic oxidation rate constant, k_p, was approximately determined from the slope of the best-fit straight line (linear regreassion) using Eq. (1) as shown in Figures 3 and 4 for both Haynes 282 and Inconel 718 at the 1050 and 1100 °C test temperatures respectively (Olivares *et al*. (2013).
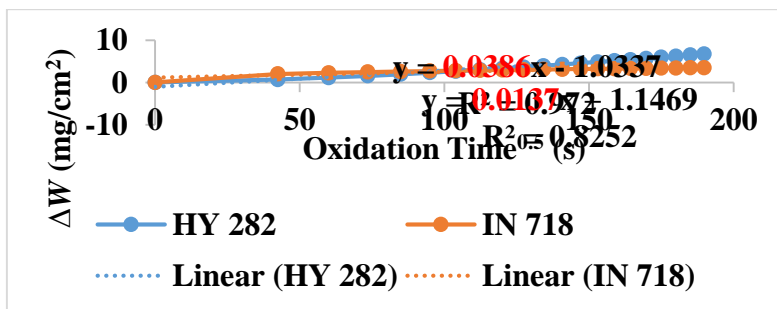
Figure 3. Plot of weight gain versus square root of exposure time for oxidation of Haynes 282 and Inconel 718 superalloys at 1050 °C.
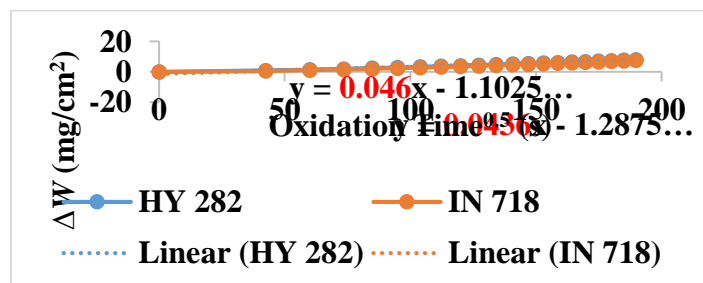

Figure 4. Plot of weight gain versus square root of exposure time for oxidation Haynes 282 and Inconel 718 superalloys at 1100 °C

The R^2 values obtained in either case show that the coefficients of determination were in good agreement with the fits. The summary of the total weight gain measurements and parabolic oxidation rate constants for both superalloys at the 1050 and 1100 °C test temperatures are shown in Table 2.

Summary of Oxidation Experiments

Table 2: Summary of oxidation kinetics of Haynes 282 and Inconel 718 superalloys at 1050 and 1100 °C test temperatures.

Alloy type	1050 °C		1100 °C	
	Total wt. gain, 36000 s (mg/cm²)	Parabolic oxidation rate constant (mg/cm². s)	Total wt. gain, 36000 s (mg/cm²)	Parabolic oxidation rate constant (mg/cm². s)
Haynes 282	20.00	3.9 x 10⁻²	24.72	4.6 x 10⁻²
Inconel 718	12.94	1.4 x 10⁻²	22.36	4.4 x 10⁻²

Weight gain as well as the parabolic oxidation rate constants were observed to increase with temperature for both Haynes 282 and Inconel 718 from 1050 to 1100 °C. Haynes 282 displayed a faster oxidation rate at both test temperatures than Inconel 718 over the whole test duration; showing a significantly higher oxidation rate at 1050 °C. The oxidation rate of Haynes 282, the slope of the fitted straight line, was approximately 3 times faster (3.9 x 10⁻² mg/cm². s) than that of Inconel 718 (1.4 x 10⁻² mg/cm². s) at 1050 °C. However, at 1100 °C, the oxidation rates of both superalloys were approximately the same as evident from curve and slope values of the best-fit straight lines.

Light Optical Microstructural Analysis

Microstructural analyses of cross-sections of the oxidized samples of both superalloys were carried out in an attempt to determine the thickness of the formed-surface-oxides. The micrographs were observed and taken at the boundary between the epoxy mount and the samples' cross-sections. Optical micrographs of the as-received superalloy test samples were taken at the 100*x* magnification.

Microstructure of as-received Haynes 282 is shown in Plate 1 (a), while that of Inconel 718 is shown in Plate 1 (b). All examined cross sections of both superalloys' oxidized samples (Plates 2 to 9, a and b) showed distinctly oxidized regions at the top external surfaces (boundary between the mount and the substrate). However, the thickness of the formed-oxide film was not readily determinable with the light optical microscope used. This could have been due to software limitation. Therefore, measurement of the oxide layer thickness from LOM was not performed in the present study to prevent inconsistency of results.
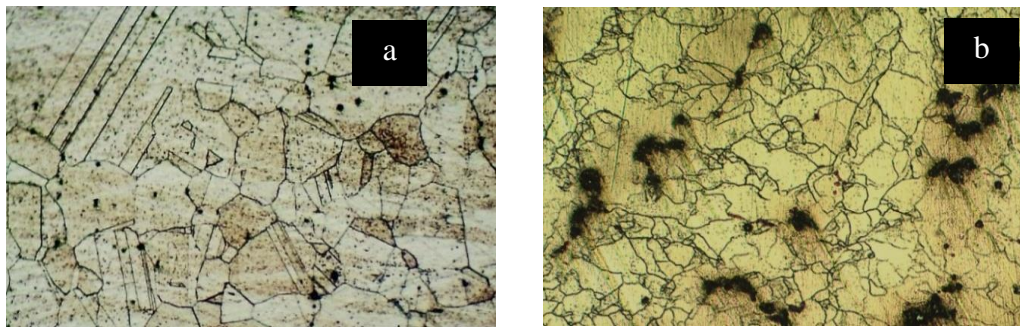
Plate 1. Optical micrographs of (a) As-Received Haynes 282 (100x), (b) As-Received Inconel 718 (100x)
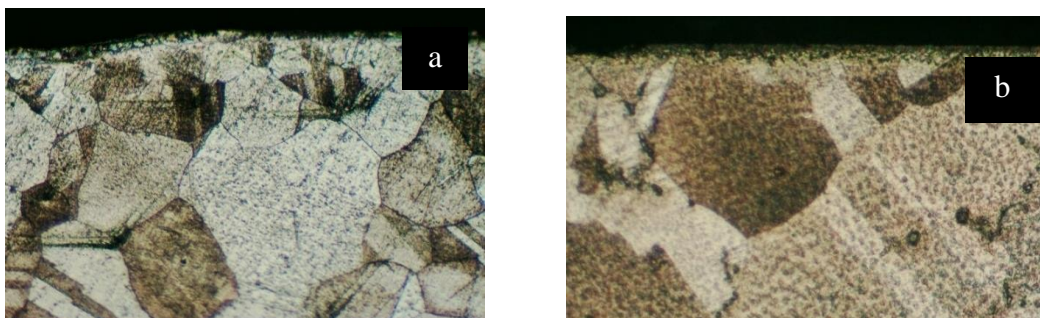
Plate 2. Optical micrographs of samples oxidized at 1050 °C for 4 hours (a) Haynes 282 Sample 1 (100x), (b) Inconel 718 Sample A (100x)
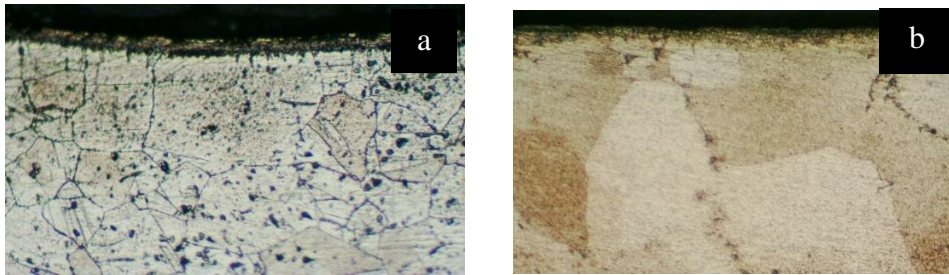
Plate 3. Optical micrographs of samples oxidized at 1050 °C for 6 hours (a) Haynes 282 Sample 2 (100x), (b) Inconel 718 Sample B (100x)
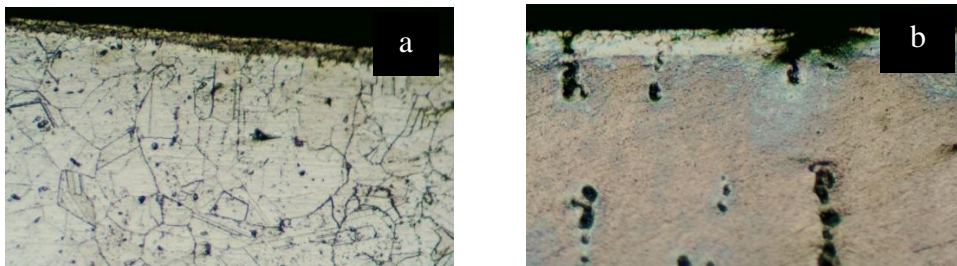

Plate 4. Optical micrographs of samples oxidized at 1050 °C for 8 hours (a) Haynes 282 Sample 3 (100x), (b) Inconel 718 Sample C (100x)
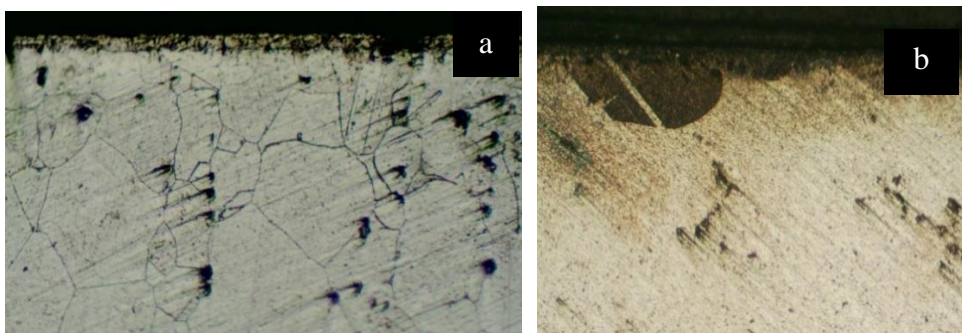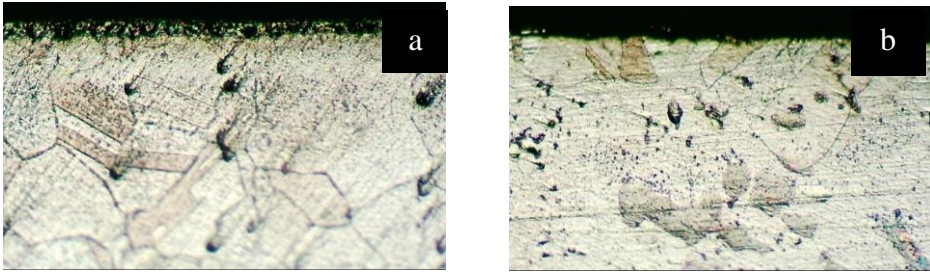

Plate 5. Optical micrographs of samples oxidized at 1050 °C for 10 hours (a) Haynes 282 Sample 4 (100x), (b) Inconel 718 Sample D (100x)

Plate 6. Optical micrographs of samples oxidized at 1100 °C for 4 hours (a) Haynes 282 Sample 5 (100x), (b) Inconel 718 Sample E (100x)
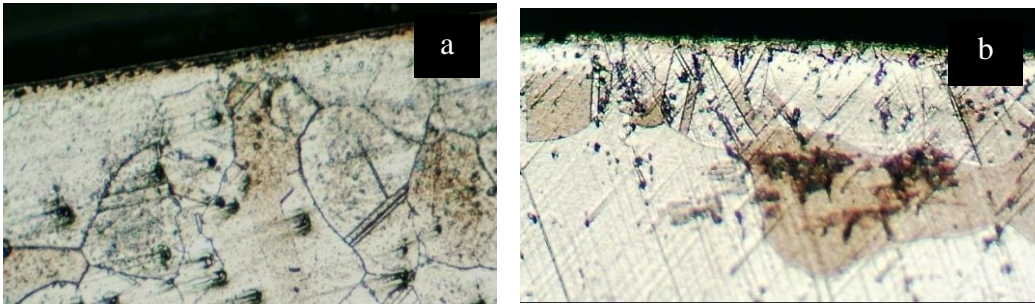

Plate 7. Optical micrographs of samples oxidized at 1100 °C for 6 hours (a) Haynes 282 Sample 6 (100x), (b) Inconel 718 Sample F (100x)
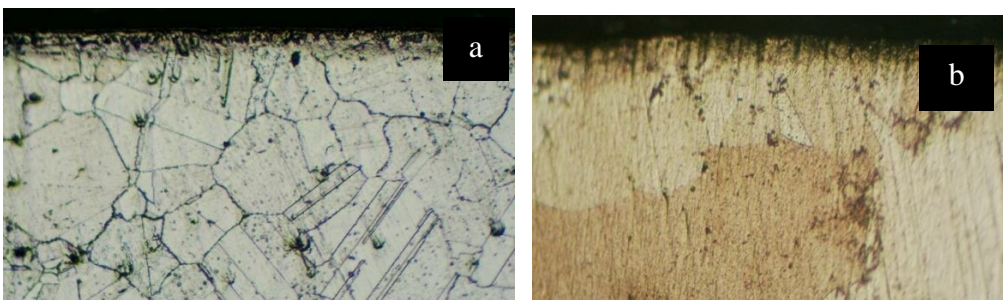

Plate 8. Optical micrographs of samples oxidized at 1100 °C for 8 hours (a) Haynes 282 Sample 7 (100x), (b) Inconel 718 Sample G (100x)
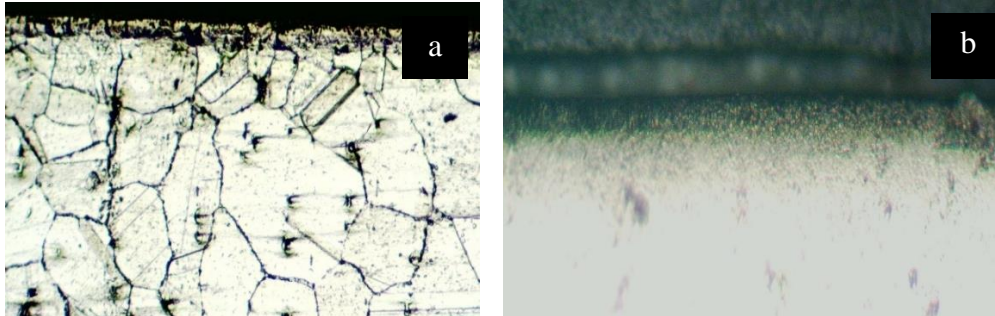
Plate 9. Optical micrographs of samples oxidized at 1100 °C for 10 hours (a) Haynes 282 Sample 8 (100x), (b) Inconel 718 Sample H (100x)

Scanning Electron Microscopy (SEM) and Energy Dispersive X-ray Spectroscopy (EDS)

In order to characterize the oxide morphology, the top surface of oxidized samples was examined using SEM. Elemental composition of the formed-surface-oxides was analysed using EDS. For this investigation, the Phenom Desktop SEM machine with Phenom ProX software attached, in Covenant University, Ota, Ogun State, Nigeria was used.

Oxidized Haynes 282 superalloy

Figures 5 and 6 show the external surface SEM image and spot EDS analysis of Haynes 282 samples oxidized at 1050 and 1100 °C for 10 hours.
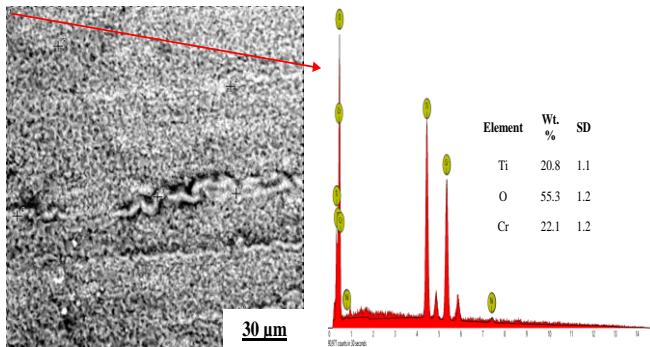

Element	Wt. %	SD
Ti	20.8	1.1
O	55.3	1.2
Cr	22.1	1.2

Figure 5. External surface SEM image of Haynes 282 sample oxidized at 1050 °C for 10 hours (2,500x) with EDS spectrum of spot 1 attached.

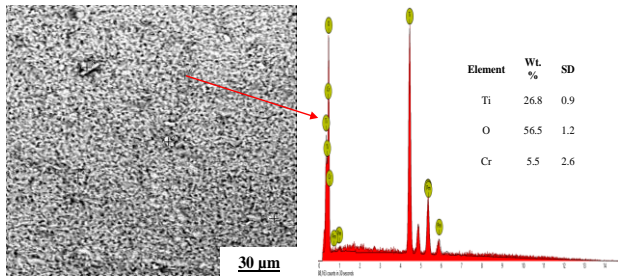| Element	Wt. %	SD
Ti	26.8	0.9
O	56.5	1.2
Cr	5.5	2.6

Figure 6. External surface SEM image of Haynes 282 sample oxidized at 1100 °C for 10 hours (2500*x*) with EDS spectrum of spot 6 attached.

Oxidized Inconel 718 superalloy

Figures 7 and 8 show the external surface SEM image and spot EDS analysis of Inconel 718 samples oxidized at 1050 and 1100 °C for 10 hours respectively.
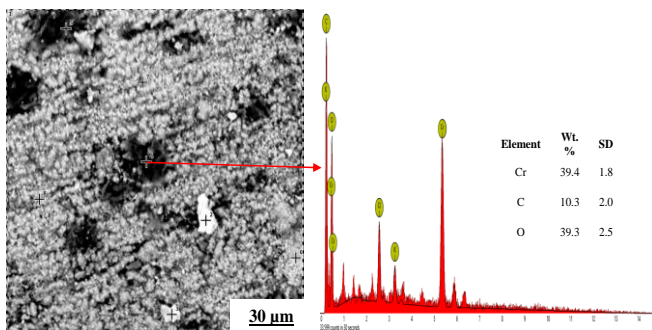

Element	Wt. %	SD
Cr	39.4	1.8
C	10.3	2.0
O	39.3	2.5

Figure 7. External surface SEM image of Inconel 718 sample oxidized at 1050 °C for 10 hours (2,500x) with EDS spectrum of spot 4 attached.

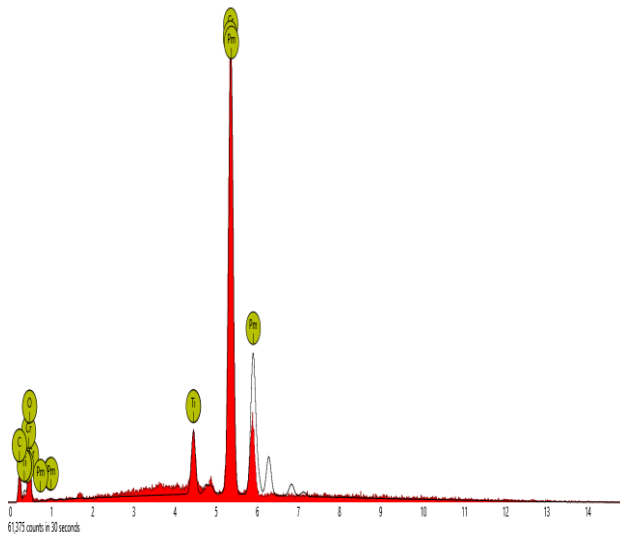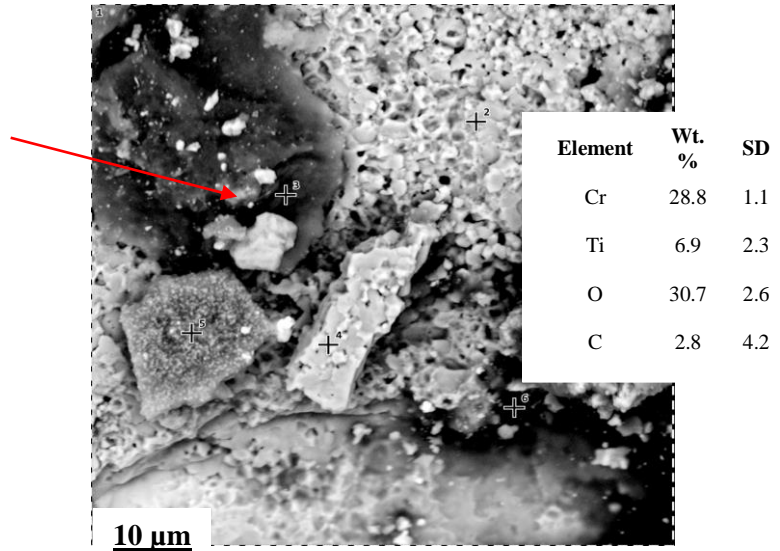| Element	Wt. %	SD
Cr	28.8	1.1
Ti	6.9	2.3
O	30.7	2.6
C	2.8	4.2

Figure 8: External surface BSD Full image of Inconel 718 sample oxidized at 1100 °C for 10 hours (5000x) with EDS spectrum of spot 2 attached.

SEM surface morphologies of Haynes 282 samples oxidized for 10 hours at 1050 and 1100 °C, as observed show crystal-like oxide structures (comparable to observations by Pérez-González *et al.* (2014); while the SEM surface morphologies of Inconel 718 samples oxidized under the same conditions as observed, show thick cluster-like oxide structures with some pores. EDS elemental composition at both

test temperatures as observed, was predominantly Cr, Ti, and O; suggesting presence of a chromium oxide film with some titanium oxide especially for Haynes 282; but predominantly chromium oxide for Inconel 718.

Generally, oxidation resistance of superalloys is fundamentally due to the formation of stable and adherent oxide layers on the materials' surfaces, which is often dependent on the oxidation reaction rate. As earlier reported, superalloys surface oxides are formed by a selective oxidation of the elements in the alloy, which is usually affected by a number of factors including relative concentration of reactive elements, cracking behaviour of the surface oxide formed, as well as an upper-temperature limit for the oxide stability before failure.

CONCLUSIONS

The following conclusions can be made from this study:
a)   At temperatures of 1050 and 1100 °C, a protective oxide film was developed on the surfaces of both Haynes 282 and Inconel 718 superalloys, which was established by the corresponding measured weight gains.

b)   Haynes 282 had a significantly faster parabolic oxidation rate, kp at 1050 $^{\circ}$C than Inconel 718; but almost the same kp at 1100 $^{\circ}$C with Inconel 718 under the same test conditions. Hence, Haynes 282 superalloy was more oxidized than Inconel 718 superalloy.

c)   At both temperatures the elemental composition of the oxide film observed on Haynes 282 suggested elemental presence of chromium oxide containing some titanium oxide-film at both test temperatures; while elemental composition of the oxide film on Inconel 718 suggested presence of predominantly chromium oxide. Both superalloys are chromia formers.

REFERENCES

Ahlatci, H. (1991). The use of coatings for hot corrosion and Erosion protection in turbine hot section components. Journal of Engineering Sciences, 5(1), 885-892.

ASM International, ASM Metals Handbook Special Volume: Heat Resistant Materials. ASM International, 1997.

Barbosa, C., Nascimento, J. L., Caminha, I.M. V., and Abud, I. C. (2005). Microstructural aspects of the failure analysis of nickel base superalloys components. Elsevier, Engineering Failure Analysis, 12, 348-361.

Caron, P. and Khan, T. (1999). Evolution of Ni-based superalloys for single crystal gas turbine blade applications. Aerospace Science Technology, 3, 513-523.

Eliaz, N., Shemesh, G. and Latanision, R. M. (2002). Hot corrosion in gas turbine components. Pergamon, Engineering Failure Analysis, 9, 31-43.

Mahobia, G. S., Sudhakar R.G., Antony, A., Chattopadhyay, K., Srinivas, N. C. S. and Singh, V. (2013). Effect of Salt Coatings on Low Cycle Fatigue Behavior of Nickel-base Superalloy GTM-SU-718. Elsevier, Procedia Engineering, 55, 830-834.

Olivares, R. I., Stein, W., and Marvig, P. (2013). Thermogravimetric study of oxidation-resistant alloys for high-temperature solar receivers. Journal of The Minerals, Metals & Materials Society (JOM-TMS), 65(12), 1660-1669.

Pérez-González, F. A., Garza-Montes-de Oca, N. F., Colás, R. (2014). High Temperature Oxidation of the Haynes 282 Nickel-based Superalloy. Springer, Oxidation of Metals, 82, 145-161.

Pollock, T M. and Tin, S. (2006). Nickel-based superalloys for advanced turbine engines: Chemistry, microstructure and properties. Journal of Propulsion and Power, 22(2), 361-374.

Pomeroy, M. J. (2005). Coatings for gas turbine materials and long-term stability issues," Materials and Design, 26(3), 223-231.

Saravanamutto, H., Rogers, G., Cohen, H., and Straznicky, P. (2009). Gas Turbine Theory, Sixth Edition ed. Edinburgh Gate, Harlow, England: Pearson Education Limited.

Shukla, V. N., Jayaganthan, R., and Tewari, V. K. (2013). Oxidation and Hot Corrosion Behaviour of Ni-based Superalloy Inconel 718 in Na2SO4-75%V2O5 Environment at Elevated Temperature. International Journal of Surface Engineering & Materials Technology, 3(1), 20-24. ISSN: 2249-7250.

Sinharoy, S. and Narasimhan, S. L. (2004). Oxidation behaviour of two nickel-base superalloys used as elevated temperature valves in spark ignited engines and

diesel exhaust recirculation (EGR) applications. Superalloys 2004, Edited by K. A. Green, T. M. Pollock, H. [14] Harada, T. E. Howson, R. C. Reed, J. J. Schirra, and S. Walston. TMS (The Minerals, Metals & Materials Society), 623-626.

Smith, M. M. (2013). Comparative Oxidation Study of Un-coated and coated CMSX-4 and CMSX-486 Single Crystal Superalloys. Masters' Thesis, University of Manitoba, Winnipeg, Canada.

The University of Manchester, Shreir's Corrosion, 4th ed., R. A. Cottis et al., Eds. Amsterdam, Netherlands: Elsevier Ltd., 2010, Vol. 1.

Wu, Y., Li, X. W., Song, G. M., Wang, Y. M., and Narita, T. (2010). Improvement of the oxidation resistance of the single-crystal Ni-based TMS-82+ superalloy by Ni–Al coatings with/without the diffusion barrier. Springer, Oxidation of Metals, 74, 287–303. DOI 10.1007/s11085-010-9211-9.

Zitnansky, M., Zrník, J., Martinkovic, M. (1998). Developing processes of property improvement of nickel base superalloys. Elsevier, Journal of Materials Processing Technology, 78, 204-209.